Journal for Re Attach Therapy and Developmental Diversities
eISSN: 2589-7799
2023 December; 6 10s(2): 2342-2354

Design, development and evaluation of Nano Based Novel Ophthalmic Drug Delivery System for Glaucoma

Monali Dumore[1]*, Praveen Sharma[2],

[1*,2]Department of Pharmacy, Oriental University, Indore, M.P

***Corresponding author:** Monali Dumore
*Department of Pharmacy, Oriental University, Indore, M.P

Abstract: In order to treat glaucoma, the in-situ gel of the chitosan nanoparticles loaded with Carteolol was developed for this investigation. By using the ionotropic gelation approach, Carteolol-loaded chitosan nanoparticles (Carteolol-CHNPs) were created. They were then further improved using the 3-factor and 3-level Box–Behnken design. Three factors were chosen as independent variables: chitosan (A), sodium tripolyphosphate (B), and stirring speed (C). They were shown to have an impact on loading capacity (LC as Y3), entrapment efficiency (EE as Y2), and particle size (PS as Y1). Gel containing nanoparticles was assessed for rheological, gelation time, gelling temperature, and transcorneal permeability. Furthermore, transcorneal permeation drug release investigations and intraocular pressure (IOP) for improved gel were carried out in vitro. Using a rabbit model, the biocompatibility of formulations was examined. Optimized Carteolol-chitosan nanoparticles are incorporated into a thermosensitive in-situ gel matrix to enhance precorneal residence time without irritating the eyes and to facilitate the sustained release of Carteolol through the cornea for efficient glaucoma treatment.

Keywords: Glaucoma, Novel, Carteolol, Ophthalmic, Chitosan, Poloxamer, Nanoparticles, In-situ gel, etc.

Introduction

Increased intraocular pressure (IOP) is a characteristic of glaucoma, the second most prevalent cause of blindness. Most of the time, an imbalance between the generation and outflow of aqueous humor through the trabecular meshwork results in the accumulation of this persistently elevated pressure in the anterior chamber of the eye. The slow death of retinal ganglion cells (RGCs) and vision impairment result from this high pressure being transferred to the posterior region of the eye, which includes the retina and optic nerve head. Tunnel vision, which leads to a gradual degeneration of the retina's ganglion cells, is a hallmark of glaucoma, often known as "The silent thief of vision." The primary risk factor is elevated intraocular pressure, which is brought on by an imbalance between the globe's drainage mechanism and the formation of aqueous humor [1]. It is the second most common cause of irreversible blindness worldwide. To achieve optimal ocular bioavailability, greater concentrations or more frequent administration of conventional dosage forms, such as suspensions and solutions, are required. However, there's a chance that this procedure will have ocular or systemic side effects. The existence of both static and dynamic barrier mechanisms lowers the drug concentration in the anterior chamber. Only 5% of the dosage that is given really reaches the ocular tissues [2]. Furthermore, overuse of preservatives like benzalkonium chloride may be harming the corneal epithelium or interfering with the effectiveness of the therapeutic medication. The medication is removed from the ocular cavity by the eye's dynamic defense systems, which include blinking, nasolacrimal drainage, and tear fluid dilution [3]. This leads to low bioavailability.

Since the eye is the most delicate organ in the body, eye drops are the most widely utilized form of treatment for ocular conditions. The eye drops' low corneal residence time (15–30 sec) and poor bioavailability (≤5%) prevent them from reaching the effective medication concentration in the ocular tissue. As a result, regular dosage is necessary to reach the therapeutic concentration. Numerous innovative ocular formulations that lengthen the corneal contact duration have been shown to improve ocular bioavailability. The application of chitosan in ocular polymeric nanoparticles to improve penetration and antibacterial activity was documented in a variety of literary works. Mucoadhesive polymers, liposomes, ocular inserts, and nanoparticles are a few of the innovative drug delivery technologies that have been employed to improve medication penetration through the corneal surface. Large ocular inserts are typically challenging to implant as non-dissolving delivery systems, which presents additional challenges. A typical nanodispersion has low viscosity, which causes the medication to be rapidly removed from the site of action by the precorneal route, resulting in poor drug availability in aqueous humor. It is challenging to introduce a viscous formulation, such as an ointment, into the eyes. The use of a hybrid system of nanoparticles loaded in situ gel is intended to address the challenges connected to ocular inserts, nanodispersion, ointments, and concerns linked to eye drops, with low drug availability in aqueous humor or other ocular tissues [4–8].

Ocular nanoparticles (NPs) can be made from a variety of natural and synthetic polymers. The capacity to increase ocular bioavailability has been tested for polymers such as chitosan, flaxseed gum, galactomannans, and eudragit RL 100. Of these, natural polymer chitosan was discovered to be an efficient, economical, and environmentally benign source of nano-carriers. A well-defined cationic polymer of the macromolecular type, chitosan (CH) is derived from

chitin. It enhances penetration and is robust, biodegradable, non-toxic, and bioadhesive. Along with hemostatic qualities that improve blood clotting, it has also demonstrated antibacterial and antifungal activity. It works on the bacteria's cell wall to have an antibacterial effect. Different cell walls are found in gram-positive and gram-negative bacteria. Compared to gram-positive bacteria, peptidoglycan on gram-negative bacteria is thinner.
The medication administration process is made easier and the residence time is extended with the use of the nanoparticulate-laden sol-gel technology. The current study's goal was to create Carteolol CHNPs using the ionotropic gelation technique. Through the use of quality by design (QbD) software, the formulation was further refined. Using polymer, the improved formulation (Carteolol -CHNPopt) was converted into a gel system. A formulation of Carteolol CHNPopt gel was assessed.

Material and Method

Materials

We received the Carteolol gift sample from Life Sciences Pvt Ltd. in Hyderabad, India. Chitosan (CH) with a low molecular weight was purchased from Sigma Aldrich. The Honeywell (Fluka Wunstorfer Strasse, Germany) provided the sodium tripolyphosphate (STP). The source of carbopol was SD-fine chemical, located in Mumbai, India. Water, acetonitrile, and methanol of HPLC grade were bought from Sigma Aldrich. Analytical grade reagents are utilized for investigation with all other chemical reagents that are obtained from the laboratory.

Method

Formulation of Carteolol Nanoparticles

The ionotropic gelation process was used to create Carteolol-loaded CH nanoparticles, or Carteolol-CHNPs. By dissolving in 1% v/v aqueous acetic acid solution and maintaining pH-5, the various CH concentration solution was created. The various STP concentrations of water were supplemented with 0.3% of Carteolol. Using a needle and a 1:2.5 ratio (STP: CH), STP solution was added drop-wise to CH solution. Carteolol (0.3%) was stirred continuously at 2500 rpm. Using a centrifuge (Remi-24, Cooling centrifuge, Mumbai, India) and a lyophilizer (Hetolyophilizer, Thermo Fisher Scientific, USA) at 100 mbar and -120 ºC, the suspension was separated. As a cryoprotectant, mannitol was employed.

Optimization

The ideal tool for optimization is Box Behnken design (BBD), which provides fewer formulations in a suitable composition. The variables were chosen using the results of an initial investigation, and the chosen variables were entered into the BBD statistical design program. Table 1 displays the three levels of the independent formulation variables (CH concentration, STP concentration, and stirring speed) at low, medium, and high. (6)

Table 1: Levels of Independent and Dependent Variables Used in Experiments

Factors	**Units**	**Level and Coded Value**		
Independent Variables		**Low (−1)**	**Medium (0)**	**High (+)**
A = Chitosan (CH)	%	0.1	0.2	0.3
B = Sodium tripolyphosphate (STP)	%	0.15	0.25	0.35
C = Stirring speed	rpm	1000	1750	2500
Dependent variables		Aim		
Y1= Particle size (PS)	nm	Minimize (< 200 nm)		
Y2= Entrapment efficiency (EE)	%	Maximize		
Y3= Loading capacity (LC)	%	Maximize		

Their impacts were noted for dependent responses such as drug loading (DL), entrapment efficiency (EE %), and particle size (PS, nm). To find the best fit model, the experimental runs were applied to a variety of kinetic models, including second-order, quadratic, cubic, and linear models. To examine the impact of independent variables on each response, the software produced a polynomial equation and three-dimensional (3D) graphs. Below is the general polynomial mathematical equation.

$Y = \beta_0 + \beta_1 A + \beta_2 B + \beta_3 C + \beta_1{}^2\, AB + \beta_1{}^3\, AC + \beta 2^{\,3}\, BC + \beta 11 A^2 + \beta 22 B^2 + \beta 33 C^2$ …….. (1)

where Y is responses, A, B, and C are the coded value of process variables, β is coefficients (linear and interaction). AB and A2 are interactions of coded variables for models.

Characterization

Particle Size and Surface characterization

Using a zeta sizer (Malvern, zeta sizer, Malvern, USA), the particle size (PS), polydispersibility index (PDI), and zeta potential (ZP) of Carteolol -CHNPs were assessed. A cuvette containing the suitably diluted material was tested at room temperature at a 90º scattering angle.

Entrapment Efficiency and Drug Load (7)

Once in the centrifugation tube, the produced Carteolol-CHNPs were centrifuged at 18,000 rpm in the cooling centrifuge (4 ºC). After separating the supernatant, the NPs pellet was cleaned with twice as much distilled water. A UV spectrophotometer set at 250 nm was used to measure the amount of Carteolol in the supernatant. The provided formula was used to compute the drug load and encapsulation efficiency.

$$EE\ (\%) = \frac{\text{Total Carteolol - Unentraaped Carteolol}}{\text{Total Carteolol}} \times 100$$

$$DL\ (\%) = \frac{\text{Total Carteolol - Unentraaped Carteolol}}{\text{Weight of NPs}} \times 100$$

Microscopic Examination

Transmission electron microscopy (JEM1011, JEOL, Inc., Peabody, MA, USA) was used to analyze the morphology of Carteolol -CHNPopt. Phosphotungstic acid (2 percent v/v) was used to stain one drop of Carteolol –CHNP opt that was deposited on the carbon-coated copper grid. The sample set aside for air drying and staining. An electronic microscope was used to examine the sample grid, and si-Viewer software was used to observe and capture the image.

X-Ray Diffraction Study (XRD)

The nature of the sample was examined using the XRD equipment (Ultima IV diffractometer, Rigaku, Japan) during the XRD investigation. The XRD sample holder was filled with the sample, which included Carteolol and lyophilized Carteolol -CHNPopt. Cu-anode was used as the radiation source, and the apparatus was run at 35 kV tube voltage and 20 mA tube current. At room temperature, the sample was scanned at a scanning rate of 1º between 5º and 70º (2 ɯ). Every spectra was captured and compared in order to assess the diffraction angle change.

Preparation of Carteolol-CHNPs loaded in situ gel

To get solution, Poloxamer 407 (13–19 w/v %) was briefly refrigerated for 8–10 hours at a temperature of 2–4°C. The polymeric solution was supplemented with Carteolol-CHNPs suspension while being stirred magnetically at 400 rpm. Additional water was added to get the desired volume.

Gelling capacity and viscosity measurement

A drop of the formulation was added to a beaker filled with 50 ml of freshly made, concentrated calcium chloride solution, and the gelling time was visually monitored in order to determine the formulation's gelling capacity. Coding according to Table 2's description of the gelling capacity. A Rheometer (Anton Paar, Austria) was used to measure the viscosity of the in situ gel. Every sample was subjected to a viscosity measurement at 37 ± 0.5°C and a constant shear rate of 100 s −1.(8)

Table 2: Coding for gelling capacity

Observation	Coding
No gelation	-
Gelation takes place within few minutes and remained for few hour	*
Immediate gelation and remained for few hour	**
Immediate gelation and for extended period	***
Very stiff gel	****

In-vitro drug release studies

Carteolol-CHNPs loaded in situ gel and in-vitro release of the commercial formulation were conducted using a diffusion cell device (Orchid Scientific, Nashik, India).In this work, a dialysis membrane-150 (Himedia, Mumbai) was used. The dialysis membrane was coated with two milliliters of in situ gel. A pH 7.4 phosphate buffer was added to the receptor compartment. A single milliliter sample was taken out on a regular basis. A UV spectrophotometer was used to measure the concentration of Carteolol at 229 nm.

Transcorneal ex vivo permeation study

A earlier description of the transcorneal ex vivo permeation investigation was given. We purchased fresh goat eyeballs from the nearby slaughterhouse. These were transported in cold, normal saline (2–3°C) from the shop to the laboratory. The cornea and 2-4 mm of the surrounding scleral portion were gently removed from the goats' eyes, and the area was then cleansed with regular saline (0.9 percent NaCl) until the most protein was gone. The removed cornea was then clamped between the donor and receptor compartments of the Franz diffusion apparatus so that the donor compartment was facing the epithelial surface and the cornea would not tear apart. The ocular region exposed for diffusion was only 1.73 cm^2. A pH 7.4 simulated tear fluid was added to the receptor compartment. A sample of about 1 milliliter was taken out on a regular basis. A UV spectrophotometer was used to measure the concentration of Carteolol at 229 nm.

In-vivo pharmacodynamics study for the evaluation of intraocular pressure

The efficacy of optimized sol in reducing intraocular pressure was investigated in white New Zealand rabbits with glaucoma (3-5 kg in weight). Over the course of seven days, they were acclimated to room temperature (25 ± 2°C) and 50 ± 15% relative humidity. Food and water were freely available to the rabbits. Steroid model produced glaucoma. The Institutional Animal Ethics Committee (IAEC), CPSEA, New Delhi (India), accepted the study. The animals were split up into three groups, with six rabbits in each. Group II was treated with optimized Carteolol-CHNPs loaded in situ gel, Group III was treated as a control, and Group I got the marketed formulation. A standardized tonometer (Nidek Non-contact tonometer) was used to measure IOP at various intervals. A 100 µl in situ gel containing 0.1% Carteolol (1 mg/ml) was infused into the left eye's conjunctival sac of the animal. IOP was estimated at various periods of time. The control eye was the right eye. The % drop in IOP at any given time point was computed using Equation (3).

$$\textbf{Percentage decrease in IOP} = \frac{\textbf{IOP Control eye} - \textbf{IOP Treated eye}}{\textbf{IOP Control eye}}$$

Ocular irritancy test

According to Organization for Economic Cooperation and Development test guideline 405, ocular irritation investigations were conducted. Three robust White New Zealand rabbits weighing between three and five kilograms were used to assess the optimized in situ gel's ocular irritancy test. The animals were kept in a room with a 12 hour light and dark cycle, 25 ± 2°C temperature, and 50 ± 15% relative humidity. Feeding was done using standard lab diets, with unlimited access to drinking water. A 100 µl in situ gel containing 0.1% Carteolol (1 mg/ml) was infused into the left eye's conjunctival sac of the animal. Using the untreated eye as a control. At 1, 24, 48, and 72 hours, the eyes were checked. The investigation came to an end if there was no sign of irritation after 72 hours. Over the course of three days, the animals were monitored at different intervals to assess the existence of any eye discomfort, as well as any redness, lesions, or corneal ulcers. There were three copies of each experiment.

In- vivo ocular tolerability effect on Hen's Egg Test Choroiallantoic Membrane (HET-CAM)

The HET-CAM assay was run using a slightly modified version of the previously published protocol. In summary, we bought fresh, viable white leghorn chick eggs from Kegg Poultry Farm and kept them in a humidified incubator with a temperature of 37 ± 0.2°C and a relative humidity of 40 ± 2%. On the third day, after aseptically drilling the egg shell, albumin (two to three milliliters) was extracted using a sterile syringe. Using a hot spatula and 70% alcohol-sterilized parafilm, the hole was sealed that same day, and the eggs were then added (equatorial position) for incubation. A appropriate window measuring 2 by 2 cm was opened on the tenth day, and 100 µl of test samples were immediately injected onto the CAM surface, allowing them to come into contact for 5 minutes. The negative control was a 0.9% NaCl solution. The test formulations were Alphagan Z ® and Carteolol-CHNPs in-situ gel, with sodium hydroxide (0.1N) acting as the positive control. For the experiment, each group used eight eggs. The scoring techniques listed in Table 3 were used to record the scores.(9)

Table 3: Scoring chart for HET-CAM test

Effect	Scores	Inference
No visible hemorrhage	0	Nonirritant
Just visible membrane discoloration	1	Mild irritant
Structures are covered partially due to membrane discoloration or hemorrhage	2	Moderately irritant
Structures are covered totally due to membrane discoloration or hemorrhage	**3**	Severe irritant

Result and Discussion

Optimization

The Box-Behnken design software was utilized to optimize Carteolol NPs, and Table 1 presents the factors that were used along with their respective concentration ranges. Table 4 illustrates the design of seventeen formulation runs with varying compositions and their corresponding responses, namely PS, EE, and DL.

Table 4: Formulation Design-Based Composition with Actual and Predicted Results of Particle Size (Nm), Entrapment Efficiency (%) and Loading Capacity (%)

Formulation Code	Independent Variables			Dependent Variables					
	A (%)	B (%)	C (rpm)	Y1 (nm)		Y2 (%)		Y3 (%)	
				Actual Value	Predicted Value	Actual Value	Predicted Value	Actual Value	Predicted Value
F1	0.1	0.15	1750	101.70	100.93	50.45	50.36	27.25	27.13
F2	0.3	0.15	1750	252.85	252.12	57.52	57.53	24.27	24.12
F3	0.1	0.35	1750	133.69	134.43	80.24	80.23	43.44	43.59
F4	0.3	0.35	1750	163.65	164.43	71.35	71.44	43.52	43.64
F5	0.1	0.25	1000	156.62	156.70	69.32	69.46	36.92	36.98
F6	0.3	0.25	1000	248.32	248.36	77.40	77.44	38.25	38.34
F7	0.1	0.25	2500	96.69	96.65	57.19	57.15	26.79	26.70
F8	0.3	0.25	2500	186.22	186.15	47.68	47.54	22.42	22.36
F9	0.2	0.15	1000	177.39	178.09	64.9	64.76	37.33	37.39
F10	0.2	0.35	1000	154.88	154.08	83.12	82.99	53.54	53.33
F11	0.2	0.15	2500	119.26	120.06	39.86	39.99	21.98	22.22
F12	0.2	0.35	2500	90.57	89.87	65.50	65.55	42.32	42.26
F13*	0.2	0.25	1750	137.65	136.45	61.04	61.16	35.05	35.20
F14*	0.2	0.25	1750	136.65	136.45	61.20	61.16	35.15	35.20
F15*	0.2	0.25	1750	133..65	136.45	61.08	61.16	35.55	35.20
F16*	0.2	0.25	1750	135.65	136.45	61.33	61.16	35.12	35.20
F17*	0.2	0.25	1750	138.65	136.45	61.17	61.16	35.14	35.20

Table 5 displays the findings of the statistical models that were fitted to the experimental runs, which included linear, second order, quadratic, and cubic models. (11,12,13)

Table 5: Statistical Model Summary for Different Kinetic Models Obtained from Design Expert Software

Response: Particle Size (Y1)						
Source (Model)	**R-Squared**	**Adjusted R2**	**Predicted R-Squared**	**Std. Dev.**	**CV (%)**	**Remark**
Linear	0.7683	0.7125	0.5349	25.94	-	-
2FI	0.8785	0.7995	0.4625	21.98	-	-
Quadratic	0.9995	0.9988	0.9973	1.59	1.07	Suggested
Entrapment Efficiency (Y2)						
Linear	0.9188	0.8978	0.8266	374.56	-	-
2FI	0.9947	0.9855	0.9623	98.35	-	-
Quadratic	0.9999	0.9999	0.9993	1.62	0.23	Suggested
Drug Loading (Y3)						
Linear	0.8912	0.8637	0.7616	281.97	-	-
2FI	0.9042	0.8406	0.4677	614.36	-	-
Quadratic	0.9997	0.9993	0.9971	3.36	0.67	Suggested

All of the responses in the design fit into a quadratic model, and no discernible difference between the actual and expected regression coefficients (R2) was found (Figure 1).

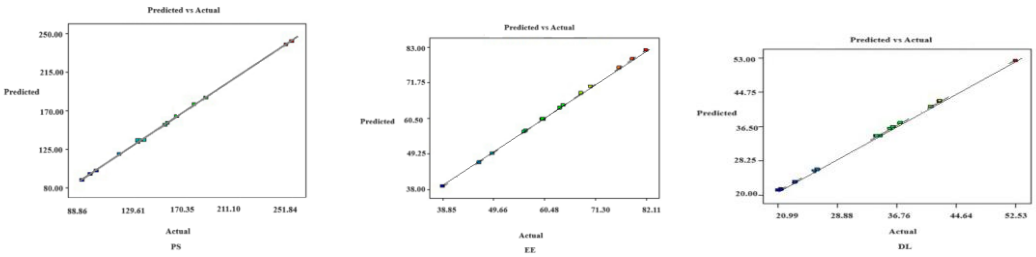

Fig. 1: Actual and predicted response of independent variables on dependent variables.

In comparison to other models, the values were found to be quite near to one another, suggesting that the model was desirable (Table 5). The fitted quadratic model's p-value of 0.05 suggested that the model was preferable. After generating the polynomial equation, it was possible to determine how each element affected each response separately and collectively. The program performed an analysis of variance (ANOVA) on each response, and the data shows that the model suited the data well (Table 6).

Table 6: Analysis of Variance of Calculated Best Fit Quadratic Model for Responses

Model	**Source**	**Particle Size (nm)**	**EE (%)**	**DL (%)**
Quadratic	Sum of Squares	33416.26	2037.34	1131.63
	df	9	9	9
	Mean Square	3713.81	227.26	126.63
	F-Value	1476.87	12137.04	2499.56
	P-value, Prob> F	<0.0001	<0.0001	<0.0001
	Remark	Suggested, significant		
Lack of fit				
Quadratic	Sum of Squares	4.5379	0.0975	0.1945
	df	3	3	3
	Mean Square	1.5127	0.0325	0.0649
	F-Value	0.4629	3.9269	1.6466
	P-value, Prob> F	0.7236	0.1099	0.3137
	Remark	Suggested, not significant		
Residual				
Quadratic	Sum of Squares	17.610	0.1306	0.3520
	df	7	7	7
	Mean Square	2.5157	0.0187	0.0503

A well-defined effect of each component on responses was displayed by the three-dimensional plot (3D-plot) that was created (Figure 2A–C).

A)

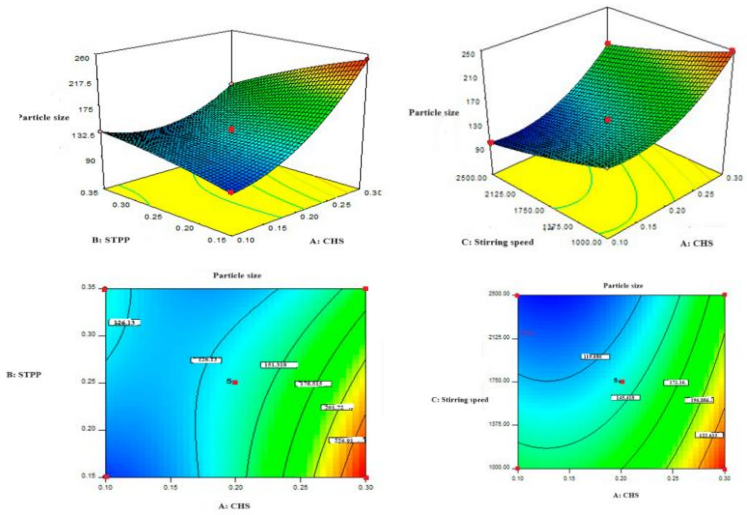

B)

C)

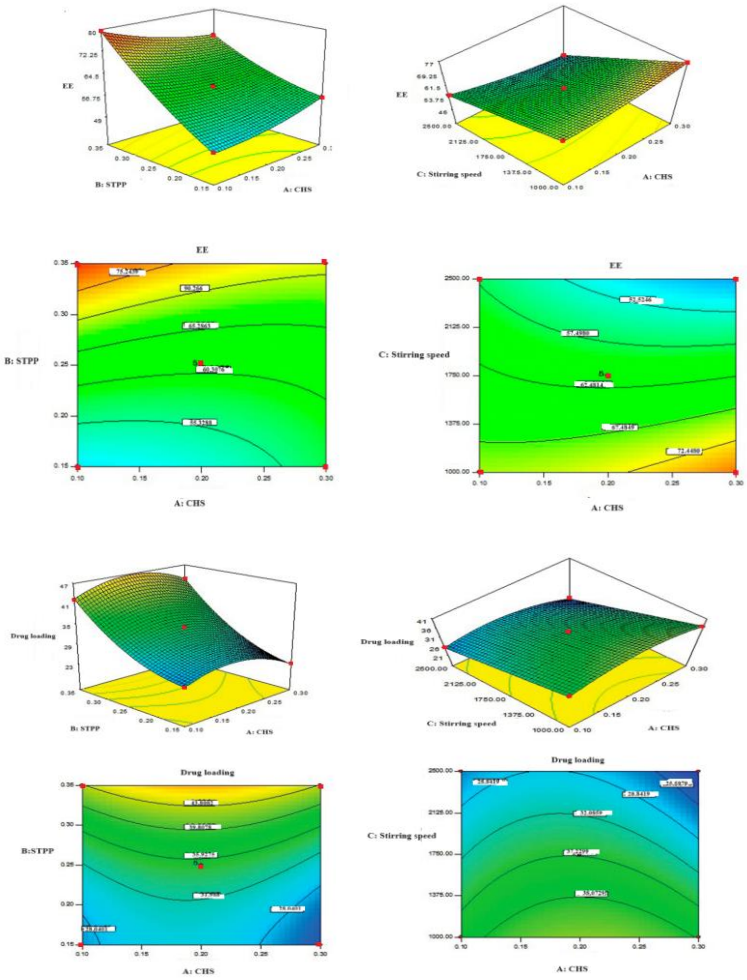

Fig. 2: Effect of independent variables A, chitosan (CH); B, sodium tripolyphosphate (STP); C, stirring speed on dependent variable ((A) size as Y1), ((B) encapsulation efficiency as Y2) and ((C) drug load as Y3)

Effect of Formulation Variables on Responses

Effect on Particle Size (PS)

Table 4 illustrates that the PS of Carteolol -CHNPs ranged from 96.69 (F7) to 252.85 nm (F2). The effect of independent variables on PS was assessed using a 3D-plot, as shown in Figure 2A. The viscosity of the CH solution rises as the concentration of CH relative to STP increases. As a result, there are more binding sites (NH2) available for cross-linking and the conductivity decreases. STP and CH are not fully cross-linked, and PS rises. Because of NP aggregation, the drop in STP concentration causes an increase in particle size. This outcome supported earlier study that was published. Stirring speed, the third variable, had a notable impact on PS. There is an inverse relationship between PS and stirring speed; that is, when the stirring speed rises from 1000 to 2500 rpm, PS falls. According to previously published work, it causes a disintegration of particles and increases the shear force. Below is the second order quadratic polynomial equation of PS as generated by the computer.

Particle size (nm Y1) = + 135:20 + 45:29 * A - 13:55 * B - 30:56 * C - 30:30 * A * B - 0:54 * A * C - 1:55 * B * C + 3 1:60 * A2 - 4:84 * B2 + 4:15 * C2 …….. (1)

The PS quadratic polynomial equation shows that stirring speed (C), STP (B), and CH (A) all had negative effects on particle size. Factors AC and BC are determined to be non-significant (P>0.05), but A, B, C, AB, A2, B2, and C2 are significant terms in the equation since they significantly affect the particle size and have a p-value of less than 0.05.

Because of the noise, the F-value is high (1476.867, indicating a significant model, P~0.0001). The model performs well, as indicated by the F-value and P-value of the lack of fit, which are 0.47 and 0.7236 (P<0.05), respectively, indicating that the lack of fit is not significant.

Table 7: Analysis of Variance of Calculated Best Fit Quadratic Model for Responses

Model	Source	Particle Size (nm)	EE (%)	DL (%)
Quadratic	Sum of Squares	33416.256	2037.34	1131.63
	Df	9	9	9
	Mean Square	3713.81	227.26	126.63
	F-Value	1476.87	12137.04	2499.56
	P-value, Prob> F	<0.0001	<0.0001	<0.0001
	Remark	Suggested, significant		
Lack of fit				
Quadratic	Sum of Squares	4.5379	0.0975	0.1945
	Df	3	3	3
	Mean Square	1.5127	0.0325	0.0649
	F-Value	0.4629	3.9269	1.6466
	P-value, Prob> F	0.7236	0.1099	0.3137
	Remark	Suggested, not significant		
Residual				
Quadratic	Sum of Squares	17.610	0.1306	0.3520
	Df	7	7	7
	Mean Square	2.5157	0.0187	0.0503

There is a fair amount of agreement between the Adjusted-R2 (0.9989) and the Predicted-R2 (0.9973). The sufficient signal for the fitted model is shown by the suitable precision of >4 (134.38).

Effect on Encapsulation Efficiency (EE)

Table 4 showed that the % EE of Carteolol -CHNPs ranged from 39.86% (F11) to 83.12% (F10). The effect of independent variables on EE was depicted by the 3D-plot, which was created (Figure 2B). The NH3 + group of CH and PO4 − of STP interact electrostatically as a result of an increase in CH viscosity. It results in decreased diffusion of Carteolol into the polymer matrix and less trapping of Carteolol into NPs. But compared to STP and stirring speed, CH had a less noticeable impact. Concentration of STP has a more pronounced positive influence on EE, meaning that an increase in concentration results in an increase in EE. It is because there are more PO4 -groups accessible for CH's NH3 + cross-linking. The more medication that during cross-linking was encapsulated or dispersed into the polymer matrix. While not as much as STP, the stirring speed has a detrimental impact on EE. Reduced EE is the result of the medication leaking from the matrix as a result of the high shear force that breaks down NPs as stirring speed increases. Below is EE's computer-generated polynomial equation for second order quadratic.

EE (Y2) = + 60:18 - 0:41 * A + 10:95 * B- 10:55 * C - 3:99 * A * B - 4:40 * A * C + 1:83 * B * C + 1:64 * A2 + 2:06 * B2 + 0:071 * C2

The polynomial equation (Equation 2)'s positive and negative signs stand for the variables' respective positive and negative effects on EE. EE was negatively impacted by CH concentration (A), meaning that a higher CH concentration results in a lower EE. The best fit was discovered to be the quadratic model. The significance of the model was indicated by the F-value of 12137.04.

The quadratic model's F and P-values of 0.47 and 0.7226, respectively, show that the lack of fit was not significant, which is favorable for a model. A sufficient precision of >4 (162.35) indicates an appropriate signal, and the predicted R2 (0.9993) and adjusted R2 (0.9999) correspond reasonably well.

Effect on Drug Load (DL)

As shown in Table 4, the DL of Carteolol -CHNPs was discovered to be between 21.99 (F11) and 53.54 % (F10). The effect of independent variables on DL was depicted in a 3D-plot that was created (Figure 2C). In the instance of CH (A), the viscosity of the CH solution rises in tandem with the concentration. It has an adverse effect on the NH3 + group's crosslinking (gelling) with PO4, which lowers DL. Stirring speed has an adverse influence on DL whereas STP (B) has a favorable effect. Because there are more binding sites (PO4 −) that cross-link with the NH3 + group of CH, DL increases as STP concentration rises. In line with earlier published studies, the more drug diffused in the polymer matrix during cross-linking and led to an increase in DL. DL is negatively impacted by stirring speed (C), as DL decreases as stirring speed increases. It results from the strong shear force breaking down of NPs and the leaching of Carteolol from NPs. The polynomial equation (Equation 3)'s positive and negative signs stand for the variables' antagonistic and synergistic effects on DL. The following is the second order computer-generated quadratic polynomial equation for DL.

Drug loading (Y3) = + 34:19 - 0:74 * A + 9:00 * B - 6:56 * C + 0:76 * A * B - 1:43 * A * C + 1:03 * B * C - 4:14 * A2 + 3:56 * B2 + 0:035 * C2

The model terms A, B, C, AB, AC, BC, A2, and B2 in this polynomial equation are important since their P-value of <0.05 shows that they are not significant. A model with acceptable precision >4 (181.96) is preferred, and the predicted R2 of 0.9971 is in reasonable agreement with the adjusted R2 of 0.9994. It was noted that the polynomial equation demonstrated the direct detrimental impact of CH.

Optimized Composition (14,15)

Carteolol -CHNPs were discovered to have a homogeneous size distribution of < 0.5 and a PS and PDI of around 200 nm. The size of the particles was determined to be within the permissible range, namely within 10 µm, which is a tolerable particle size for ocular instillation. Carteolol-CHNPopt (composition: CH 0.2%, STP 0.25%, stirring speed: 1750 rpm) had PS and PDI measurements of 144.4 nm and 0.114 ± 0.015, respectively (Figure 3A). Carteolol -CHNPopt was discovered to have a positive and high zeta potential of 26.2 mV (Figure 3B), indicating that the dispersion of NPs is both stable and non-aggregated.

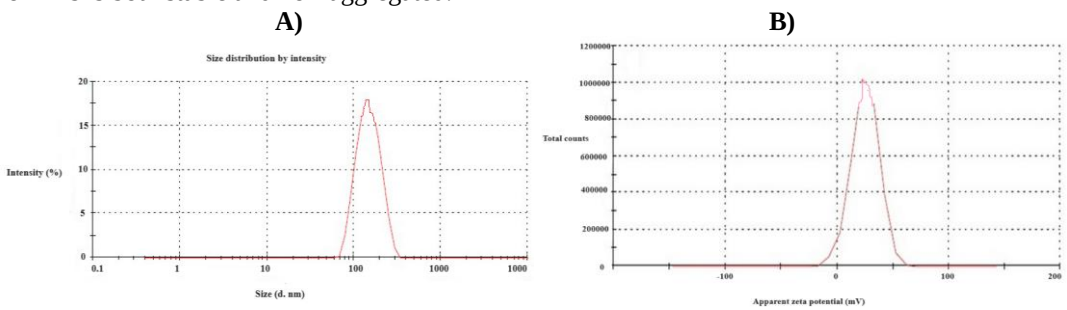

Fig. 3: Particle size (A) and Zeta potential (B) of optimized Carteolol chitosan nanoparticles

Carteolol -CHNPopt was discovered to have an EE of 61.19 ± 2.66 % and a DL of 35.20 ± 1.88 %. TEM analysis provided additional confirmation of Carteolol -CHNPopt's shape, revealing smooth, spherical surface particles free of aggregation (Figure 4).

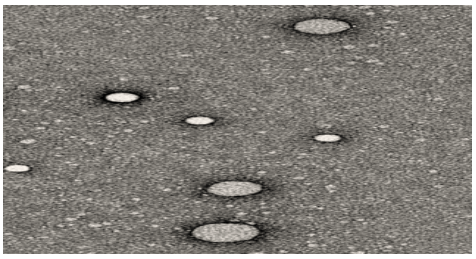

Fig.4: Transmission electron microscopic image of optimized Carteolol chitosan nanoparticles

X-Ray Diffraction Study (XRD)

To assess the crystallinity, spectral analysis was done on both lyophilized Carteolol CHNPopt and pure Carteolol. Carteolol XRD spectra revealed a high distinctive peak at 2 theta value, which shows its crystallinity. The values are 38.0º (d-2.3660) and 44.2º (d-2.0474) (Figure 5A). Additionally, lyophilized Carteolol -CHNPopt only displayed the distinctive CH peak at 2 theta value 19.2º (d-4.6189), indicating a decrease in GTM crystallinity (Figure 5B). It suggests that the drug Carteolol was entirely dissolved or encased in chitosan and dispersed in an erratic manner.(16,17)

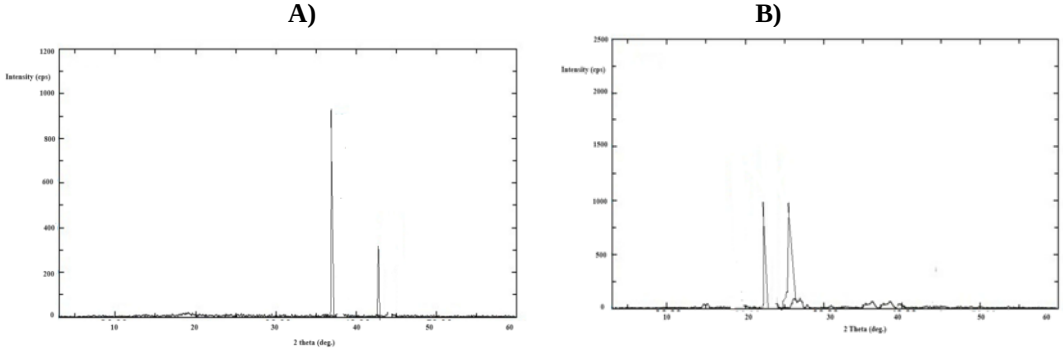

Fig. 5: XRD of (A). Carteolol and (B). Optimized Carteolol chitosan nanoparticles

Journal for Re Attach Therapy and Developmental Diversities
eISSN: 2589-7799
2023 December; 6 10s(2): 2342-2354

Evaluation of Carteolol CHNPopt loaded in situ gel

It was decided to use a viscosity modifier (Poloxamer) and a thermo responsive in situ gelling polymer to improve the flow characteristics and gelling behavior of the final product while reducing the total polymer load. Different Poloxamer-407 concentrations were utilized and their gelling capacities were measured in order to test suitable formulations for in situ gels. Given that it stays in sol form at 37°C, formulation (F-1) with the lowest polymer content demonstrated a limited gelling capacity with "*" grade gel (Table 8). Formulation (F-2) containing 15% Poloxamer-407 gels at 39.5°C, which is much higher than the physiological temperature, exhibiting ** grade of gelling capacity. A *** grade gel was prepared using a formulation that contained 17% Poloxamer-407 (F-3), gelling at a temperature that is close to body temperature (36.9°C). The **** grade of gelling capacity is exhibited by formulation (F-4) with 19% Poloxamer-407, which gels at 31°C, a temperature that is significantly lower than physiological. Based on these results, it can be concluded that concentration has a significant influence on Poloxamer gel's thermo responsiveness. Rapid gelation is achieved at a lower gelation temperature when a higher concentration of Poloxamer 407 is used. To prevent quick removal by tearing, the sol should ideally gel promptly or very quickly upon exposure to its gelation temperature. Formulation F-1 takes the longest to gel; Table 8 shows that this is clearly due to the lower concentration of Poloxamer 407. Because Formulation F-4 has a high amount of Poloxamer 407, it gels relatively quickly—about 16 seconds. The findings indicated that a lower sol-gel transition temperature is linked to a higher amount of Poloxamer and a shorter gelation period. F-3 formulations were chosen for additional analysis based on the following factors: viscosity, gelling capability, gelation time, and temperature. The outcomes demonstrated that gels with higher amounts of Poloxamer formed stiff structures due to their enhanced network.(18,19,20)

Table 8: Evaluation of various Carteolol CHNP opt loaded in situ gel

Formulation	Poloxamer-407 (%w/v)	Gelation time (s)	Gelling capacity	Gelling temperature (°C)	Viscosity (cps)
F1	13	35.26 ± 2.52	*	44.41 ± 1.22	58.13 ± 12.45
F2	15	28.51 ± 1.24	**	40.51 ± 2.15	129.90 ± 6.94
F3	17	22.51 ± 2.64	***	37.91 ± 1.31	694.18 ± 13.16
F4	19	17.76 ± 0.59	****	32.01 ± 0.24	812.74 ± 16.64

In vitro drug release

Figure 6a displays the in vitro drug release characteristics of commercial formulations and optimized nanoparticle solution loaded in situ gel. Because the marketed eye drops contained less viscosity, they diffused quickly into the release media (two hours). Within two hours, the total amount of released Carteolol from marketed eye drops was 97.99 ± 3.92%, whereas within twenty-four hours, the total amount released from optimized preparation was 86.32 ± 3.52%. As anticipated, a controlled drug delivery system might be used using Carteolol CHNP opt loaded in situ gel. After fitting in vitro release data of a commercial formulation, the correlation coefficients obtained show that a zero-order model provided the greatest fit. The zero-order model had the highest correlation coefficient value (R2 = 0.994). The two drug release phenomena—diffusion of the drug from the nanoparticle core and drug dissolution in the particle core—may be responsible for sustained and continuous release. Because of the superior emulsifying properties and heavy character of vitamin E TPGS, the improved formulation demonstrated a more prolonged and sustained activity when compared to the marketed formulation. Furthermore, the emulsifying ability of Vitamin E TPGS prolongs the drug's contact duration and enhances its residence period. The hydrophobic qualities of PLGA and the waxy nature of TPGS regulated the drug's penetration from the polymer matrix in the medium. The observation revealed that the drug release kinetics followed a mixed release kinetics pattern, with R 2 = 0.983 for zero order, R 2 = 0.990 for Higuchi's release kinetics, and R 2 = 0.997 for the Korsemeyer-Peppas drug release model. Drug release, drug movement, and the creation of fine channels are all caused by the drug release medium's entry into the polymer matrix. In a nutshell, the way that Carteolol is released can be described as follows: the drug release medium enters the matrix of nanoparticles, dissolves the Carteolol, and then forms fine channels (a porous network). Carteolol that has been dissolved spreads via the tiny channels.

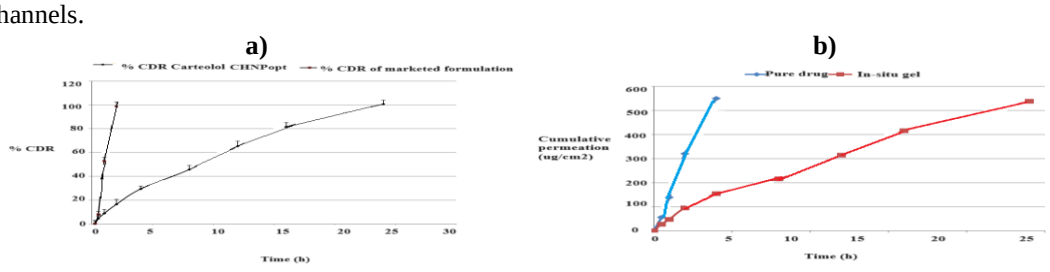

Fig.6: (a) Release profile and (b) transcorneal ex-vivo study of Carteolol from marketed eye drop and optimized Carteolol CHNP loaded in situ gel. Data show mean ± SD (n = 4).

Transcorneal permeation study

To investigate the ex vivo permeability of Carteolol commercialized and optimized Carteolol CHNP opt integrated in situ gel, transcorneal permeation studies were conducted on excised corneas of goat eyes (Figure 6b). The in situ gel's transcorneal steady-state flow in 4 hours was 137.33 µg cm−2 h−1, while the commercially available Carteolol showed a flux of 39.61 µg cm−2 h−1, which is around 3.5 times greater than the commercial formulation. These findings demonstrated that the gel matrix allowed a constant level of Carteolol to infiltrate into the cornea. This could be explained by the in situ gel's transition temperature, which is 37°C. As a result, this trait of it may have a significant influence on Carteolol's ability to pass through the cornea.

In-vivo pharmacodynamics study for evaluation of IOP

A commercial formulation and the anti-glaucomatic impact of optimized nanoparticles added in situ gel were compared. The relationship between time and IOP reduction was assessed. The average change in IOP between the treated and control eyes was used to express the ocular antihypertensive effect (Figure 7a). For the marketed pharmacological product, an average difference in IOP of 3.4 ± 0.26 mmHg was found after 30 minutes; at 8 hours, the difference gradually declined to 3.9 ± 1.02 mmHg ($p < .01$). However, the optimized nanoparticles placed into the in situ gel exhibit a more regulated and efficient mode of action. The pharmacological effect of Carteolol was observed for 8 hours ($p < .01$), during which a constant decrease in IOP of 9.7 ± 0.86 mmHg was noted for the nanoparticles loaded in situ gel. After 30 minutes, the IOP had decreased by 9.09 ± 1.26 mmHg. Carteolol CHNP opt in situ gel's percentage IOP decrease (35.47 ± 4.22%) was greater than that of the commercial formulation (13.25 ± 3.0 %) up until 8 hours ($p < .01$). When compared to a commercial eye drop, it was clear that the nanoparticles loaded in situ gel demonstrated a significant IOP lowering action over an extended period of time. Because the marketed eye drop is less viscous, it does not stick to cul de sac; yet, thermosensitive nanogel lengthens the drug's precorneal residence time in the cornea and provides sustained action for a longer period of time.

a)

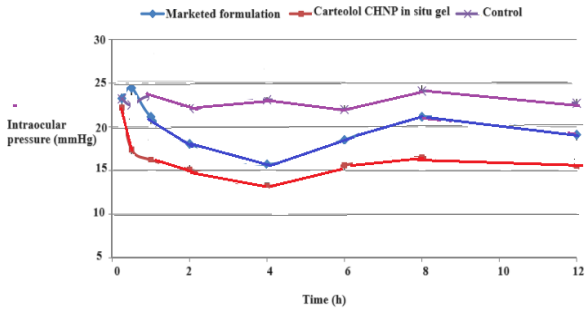

b)

Marketed eye drop

Day 0 **Day 1** **Day 2** **Day 3**

Nanoparticles loaded in-situ gel

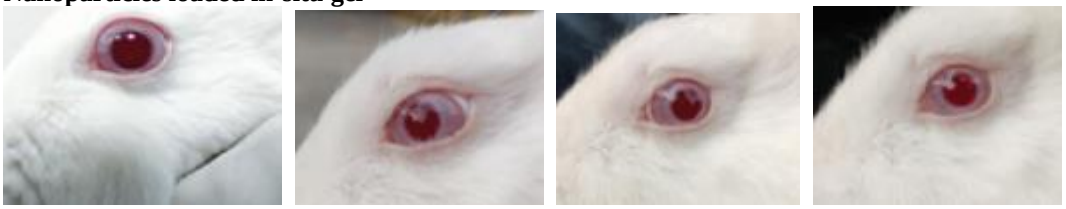

Fig. 7: IOP activity of marketed formulation and Carteolol CH loaded nanoparticles incorporated in situ gel (Mean ± SD, n = 5). (b) Appearance of rabbit eyes treated with 100 µL of (a) marketed eye drop (0.1%) and (b) nanoparticles loaded in situ gel.

Ocular irritancy test

Albino rabbits had an optimal formulation injected into their left eye, and the animals were observed for three days. The refined formulation with a zero score on the redness scale was deemed non-irritating and non-corrosive. To confirm the results, the experiment was conducted on two more animals. Over the course of three days, no animal displayed signs of eye damage, according to the study (Figure 7b). As a result, the optimized nanoparticles included in situ gel were safe for application in the eyes, non-irritating, and non-corrosive. (21-24)

Ocular tolerability test (HET-CAM test)

The produced Carteolol CHNP opt loaded in-situ gel was tested using the HET-CAM method to determine its irritation potential and tolerability. The results were compared between the positive control (0.1 N NaOH) and the negative control (0.9 % w/v normal saline). When compared to the positive control and marketed formulation, the test and negative control formulations were categorized by mean scores as non-irritant. For the test formulation and normal saline, a mean score of 0 was achieved. Compared to the positive control, the optimized Carteolol CHNP loaded in-situ gel did not exhibit any signs of lysis or coagulation after five minutes. As seen in Figure 8, the study demonstrates that the test formulation is well tolerated for ocular distribution for up to eight hours and is safe and nonirritating.(25,26)

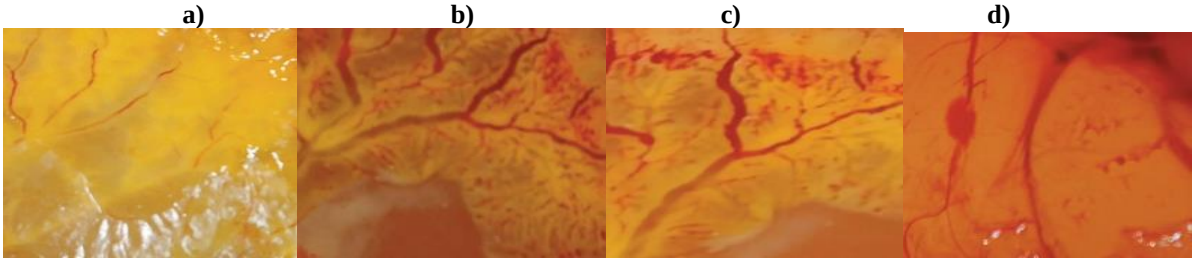

Fig. 8: (a) CAM treated normal saline (0.9% w/v), (b) CAM treated with 0.1M NaOH, (c) treatment of CAM with Carteolol CHNP loaded in-situ gel, and (d), Alphagan Z ® treated CAM

Conclusion

Using box-Behnken statistical design, chitosan nanoparticles of Carteolol were effectively synthesized and optimized. The Carteolol-CHNPs that were synthesized had a positive zeta-potential and a particle size of less than 200 nm. Optimized Carteolol-CHNPs were placed onto a thermosensitive in situ gel based on Poloxamer 407, depending on the results mentioned above. When the temperature was raised to 37°C, the Nanoformulation quickly gelled (20 s) from a liquid state. By prolonging the precorneal residency period due to its mucoadhesive feature, the optimized nanoparticles loaded in situ gel were able to sustain drug release for up to 24 hours, as shown by the in vitro release experiments. This is in contrast to commercialized eye drops. Up to eight hours ($p < .01$), the in situ gel version of Carteolol-CHNPs' IOP reduction percentage (35.47 ± 4.22 %) was roughly three times more than that of the commercial formulation (13.25 ± 2.91 %). The ocular eye irritation investigation found that the produced gel did not cause redness or ocular irritation in the animal model, in accordance with OECD criteria. Thus, the statistically tailored Nanoformulation may be a viable delivery system for Carteolol, enabling better glaucoma therapy through increased efficacy and patient adherence.

References

1. V. Mishra. Acetazolamide encapsulated dendritic nano-architectures for effective glaucoma management in rabbits. Int. J. Pharm. 2014. 34:786-98.
2. L. Lalu. Novel nanosystems for the treatment of ocular inflammation: current paradigms and future research directions J. Contr. Release. 2017; 3(2):678-84.
3. N. Thomas. In vitro and in vivo performance of novel supersaturated self-nanoemulsifying drug delivery systems (super-SNEDDS). J. Contr. Release. 2012; 65:876.
4. Barse R., Kokare C., Tagalpallewar A. Influence of hydroxyl propyl methylcellulose and poloxamer composite on developed ophthalmic in situ gel: ex vivo and in vivo characterization. J Drug Deliv Sci Technol. 2016; 33:66–74.
5. Addepalli UK., Jonnadula GB., Garudadri CS., Khanna RC., Papas EB. Prevalence of primary glaucoma as diagnosed by study optometrists of L. V. Prasad eye institute–glaucoma epidemiology and molecular genetics study. Ophthalmic Epidemiol. 2019; 26 (3):150–54.
6. Barse RK., Tagalpallewar AA., Kokare CR., Sharma JP., Sharma PK. Formulation and ex vivo–in vivo evaluation of PH-triggered brimonidine tartrate in situ gel for the glaucoma treatment using application of 32 factorial design. Drug Dev Ind Pharm. 2018; 44 (5):800–07.
7. Morsi N., Ghorab D., Refat H., Teba H. Ketoroloac tromethamine loaded nanodispersion incorporated into thermosensitive in situ gel for prolonged ocular delivery. Int J Pharm. 2016; 506(1–2):57– 67.

8. Silva AC., Amaral MH., González-Mira E., Santos D., Ferreira D. Solid Lipid Nanoparticles (SLN) - Based hydrogels as potential carriers for oral transmucosal delivery of risperidone: preparation and characterization studies. Colloids Surfaces B Biointerfaces. 2012; 93:241–48.
9. Bateman DN, Clark R, Azuara-Blanco A, Bain M, Forrest J. The effects of new topical treatments on management of glaucoma in Scotland: an examination of ophtalmological health care. Br J Ophtalmol. 2002;86(5):551–4.
10. Kastrup EK. Drug facts and comparisons. USA: Wolters Kluwer Health; 2012. p. 3193–4.
11. Kaur IP, Aggarwal D, Singh H, Kakkar S. Improved ocular absorption kinetics of timolol maleate loaded into a bioadhesive niosomal delivery system. Graefes Arch Clin Exp Ophthalmol. 2010;248(10):1467–72.
12. Kouchak M. In situ gelling systems for drug delivery. Jundishapur J Nat Pharm Prod. 2014;9(3):e20126.
13. Lin H, Sung KC. Carbopol®/pluronic phase change solutions for ophthalmic drug delivery. J Control Release. 2000;69:379–88.
14. Srividya B, Cardoza RM, Amin PD. Sustained ophthalmic delivery of ofloxacin from a pH triggered in situ gelling system. J Control Release. 2001;73(2–3):205–11.
15. Gupta S, Vyas SP. Carbopol/chitosan based pH triggered in situ gelling system for ocular delivery of timolol maleate. Sci Pharm. 2010;78(4):959–76.
16. Moiseev RV, Steele F, Khutoryanskiy VV. Polyaphron formulations stabilised with different water-soluble polymers for ocular drug delivery. Pharmaceutics. 2022;14(5):926. doi: 10.3390/pharmaceutics14050926.
17. Radomska-Soukharev A, Wojciechowska J. Microemulsions as potential ocular drug delivery systems: phase diagrams and physical properties depending on ingredients. Acta Pol Pharm. 2005;62(6):465–471.
18. . Doshi U, Xu J. Effect of viscosity, surface tension and mucoadhesion on ocular residence time of lubricant eye drops. Invest Ophthalmol Vis Sci. 2009;50(13):4641–4641.
19. Luo Q, Zhao J, Zhang X, Pan W. Nanostructured lipid carrier (NLC) coated with Chitosan Oligosaccharides and its potential use in ocular drug delivery system. Int J Pharm. 2011;403(1–2):185–191. doi: 10.1016/j.ijpharm.2010.10.013.
20. Stahl U, Willcox M, Stapleton F. Osmolality and tear film dynamics. Clin Exp Optom. 2012;95(1):3–11. doi: 10.1111/j.1444-0938.2011.00634.x.
21. Murube J. Tear osmolarity. Ocul Surf. 2006;4(2):62–73. doi: 10.1016/S1542-0124(12)70028-9.
22. Varela-Fernández R, Díaz-Tomé V, Luaces-Rodríguez A, et al. Drug delivery to the posterior segment of the eye: biopharmaceutic and pharmacokinetic considerations. Pharmaceutics. 2020;12(3):269. doi: 10.3390/pharmaceutics12030269.
23. Shetty R, Naidu JR, Nair AP, et al. Distinct ocular surface soluble factor profile in human corneal dystrophies. Ocul Surf. 2020;18(2):237–248. doi: 10.1016/j.jtos.2019.11.007.
24. Romeo A, Musumeci T, Carbone C, et al. Ferulic acid-loaded polymeric nanoparticles for potential ocular delivery. Pharmaceutics. 2021;13(5):687. doi: 10.3390/pharmaceutics13050687.
25. Carnevale C, Riva I, Roberti G, et al. Confocal microscopy and anterior segment optical coherence tomography imaging of the ocular surface and bleb morphology in medically and surgically treated glaucoma patients: a review. Pharmaceuticals (Basel) 2021;14(6):581. doi: 10.3390/ph14060581.
26. Khalil IA, Ali IH, El-Sherbiny IM. Noninvasive biodegradable nanoparticles-in-nanofibers single-dose ocular insert: in vitro, ex vivo and in vivo evaluation. Nanomedicine (Lond) 2019;14(1):33–55. doi: 10.2217/nnm-2018-0297.